Magnetic properties of $Ho_{0.9}Er_{0.1}Fe_3(BO_3)_4$

Magnetic properties of $Ho_{0.9}Er_{0.1}Fe_3(BO_3)_4$

Irina Gudim[1], Andrey Demidov[2], Eugene Eremin[1,3], Vladislav Temerov[1] and Dinesh Shukla[4]

[1] Kirensky Institute of Physics, SB RAS, 660036 Krasnoyarsk, Russia
[2] Bryansk State Technical University, 241035 Bryansk, Russia
[3] Siberian Federal University, 660041 Krasnoyarsk, Russia
[4] UGC-DAE Consortium for Scientific Research, 452017 Indore, India

E-mail: irinagudim@mail.ru

Abstract. The magnetic properties of $Ho_{0.9}Er_{0.1}Fe_3(BO_3)_4$ ferroborate with the competing Ho–Fe and Er–Fe exchange couplings have been experimentally and theoretically investigated. The measured magnetic characteristics ($M_{a,c}(B)$, $\chi_{a,c}(T)$) and observed features are interpreted using a single theoretical approach based on the molecular-field approximation and calculations within the crystal-field model of the rare-earth ion. Interpretation of the experimental data includes determination of the crystal-field parameters for Ho^{3+} and Er^{3+} ions in $Ho_{0.9}Er_{0.1}Fe_3(BO_3)_4$ and parameters of the Ho–Fe and Er–Fe exchange couplings.

1. Introduction

The rare-earth borates $RM_3(BO_3)_4$ (R = Y or La–Lu and M = Al, Sc, Cr, Fe and Ga) exhibit a vast diversity of magnetic, magnetoelectric, magnetoelastic and other physical properties [1, 2]. An increased interest in the borates $RM_3(BO_3)_4$ is due to the possibility of studying the substituted $R_{1-x}R'_xFe_3(BO_3)_4$ compositions, where the presence of competing R–Fe and R'–Fe exchange couplings can ensure the occurrence of spontaneous reorientation transitions [3-5]. The iron magnetic moments in $HoFe_3(BO_3)_4$ are antiferromagnetically ordered at $T_N \approx 38$–39 K and, with a decrease in temperature to $T_{SR} \approx 4.7$–5 K, lie in the *ab* basal plane, similar to the magnetic moments of Ho^{3+} ions [6]. At $T_{SR} \approx 4.7$–5 K, the spontaneous spin-reorientation transition occurs; as a result, the magnetic moments of the Ho- and Fe-subsystems align parallel to the *c*-axis. In $ErFe_3(BO_3)_4$ at $T < T_N \approx 38$ K, all magnetic moments lie in the *ab* basal plane [1, 7]. In $YFe_3(BO_3)_4$ at $T < T_N \approx 37$ K, the magnetic moments of Fe lie in the basal plane *ab* [1, 7]. Thus, the competition of contributions of the Ho-, Er- and Fe-subsystems to the magnetic anisotropy of $Ho_{1-x}Er_xFe_3(BO_3)_4$ can result in the occurrence of the spontaneous and magnetic field-induced spin-reorientation transitions. These transitions were observed for $Ho_{1-x}Nd_xFe_3(BO_3)_4$ [4, 8] and $Nd_{1-x}Dy_xFe_3(BO_3)_4$ [3].

In this work the experimental and theoretical investigations of the field and temperature dependences of magnetization $M_{a,c}(B)$ and the temperature dependences of the magnetic susceptibility $\chi_{a,c}(T)$ of $Ho_{0.9}Er_{0.1}Fe_3(BO_3)_4$ have been performed.

2. Experiment

The $Ho_{0.9}Er_{0.1}Fe_3(BO_3)_4$ single crystals were grown from fluxes based on bismuth trimolibdate 78 wt. % [$Bi_2Mo_3O_{12}$ + $3B_2O_3$ + $0.45Ho_2O_3$ + $0.05Er_2O_3$] + 22 wt. % $Ho_{0.9}Er_{0.1}Fe_3(BO_3)_4$ by the technique described in detail in [9, 10].

The magnetic measurements were performed on a Quantum Design Physical Property Measurement System in the temperature range of 3–300 K and magnetic fields of up to 9 T.

3. Theory

The magnetic properties of $Ho_{0.9}Er_{0.1}Fe_3(BO_3)_4$ crystals are determined both by the magnetic subsystems and by the interaction between them. The Fe-subsystem in this compound can be considered as consisting of two antiferromagnetic sublattices. The rare-earth subsystem (magnetized due to the *f–d* interaction) can also be represented as a superposition of two sublattices. In the calculations, we used a theoretical approach which has been applied for description of the magnetic properties of the $RFe_3(BO_3)_4$ (see e.g. [2, 5, 8]). This approach is based on a crystal-field model for the R-ion and on the molecular-field approximation. Effective Hamiltonians describing the interaction of each R/Fe ion in the *i*th (*i* = 1, 2) sublattice of the corresponding subsystem in the applied magnetic field B can be written as

$$\mathcal{H}_i\left(\mathrm{R}\right) = \mathcal{H}_i^{\mathrm{CF}} - g_J^{\mathrm{R}}\mu_B\,\mathbf{J}_i^{\mathrm{R}}\left[\mathbf{B} + \lambda_{fd}^{\mathrm{R}}\,\mathbf{M}_i^{\mathrm{Fe}}\right], \tag{1}$$

$$\mathcal{H}_i\left(\mathrm{Fe}\right) = -g_S\mu_B\,\mathbf{S}_i\left[\mathbf{B} + \lambda\,\mathbf{M}_j^{\mathrm{Fe}} + \left(1-x\right)\lambda_{fd}^{\mathrm{Ho}}\,\mathbf{m}_i^{\mathrm{Ho}} + \; + x\lambda_{fd}^{\mathrm{Er}}\,\mathbf{m}_i^{\mathrm{Er}}\right],\; j = 1,\quad 2,\quad j \neq i, \tag{2}$$

where $\mathcal{H}_i^{\mathrm{CF}}$ is the crystal-field Hamiltonian (see e.g. [8]), g_J is the Lande factor, $\mathbf{J}_i$ is the operator of the angular moment of the R-ion, $g_S = 2$ is the *g*-value, $\mathbf{S}_i$ is the operator of the spin moment of an iron ion, $\lambda_{fd} < 0$ and $\lambda < 0$ (including intrachain $\lambda_1 < 0$ and interchain $\lambda_2 < 0$) are the molecular constants of the antiferromagnetic interactions R–Fe and Fe–Fe, respectively. The magnetic moments of the *i*th iron $\mathbf{M}_i^{\mathrm{Fe}}$ and rare-earth $\mathbf{m}_i^{\mathrm{R}}$ sublattices per formula unit are defined as

$$\mathbf{M}_i^{\mathrm{Fe}} = 3g_S\mu_B\left\langle\mathbf{S}_i\right\rangle,\; \mathbf{m}_i^{\mathrm{R}} = g_J^{\mathrm{R}}\mu_B\left\langle\mathbf{J}_i^{\mathrm{R}}\right\rangle. \tag{3}$$

In order to calculate the magnitudes and orientations of magnetic moments in the Fe- and R-subsystems, it is necessary to solve a self-consistent problem based on Hamiltonians (1, 2) under the condition of minimum for the corresponding thermodynamic potential (see e.g. [5, 8]). Then, it is possible to determine the regions of stability of various magnetic phases, the critical fields for the phase transitions, the magnetization curves, magnetic susceptibilities, etc.

The magnetization and magnetic susceptibility of the compound (per f.u.) are defined as

$$\mathbf{M} = \frac{1}{2}\sum_{i=1}^{2}\left(\mathbf{M}_i^{\mathrm{Fe}} + \left(1-x\right)\mathbf{m}_i^{\mathrm{Ho}} + x\,\mathbf{m}_i^{\mathrm{Er}}\right), \tag{4}$$

$$\chi_k = \chi_k^{\mathrm{Fe}} + \left(1-x\right)\chi_k^{\mathrm{Ho}} + x\chi_k^{\mathrm{Er}},\quad k = a,\; b,\; c\,. \tag{5}$$

4. Results and discussion

In order to determine the parameters of the crystal-field we have used the experimental data on the temperature dependence of the magnetic susceptibility $\chi_{a,c}(T)$, the field and temperature dependences of the magnetization $M_{a,c}(B, T)$ and existing information on the structure of the ground multiplet of Ho^{3+} ion in $HoFe_3(BO_3)_4$ and Er^{3+} ion in $ErFe_3(BO_3)_4$. The initial values of the crystal-field parameters, from which the procedure of minimization of the corresponding target function was started, were selected from the values available for ferroborates: $HoFe_3(BO_3)_4$ [11], $ErFe_3(BO_3)_4$ [11] and $Ho_{0.5}Nd_{0.5}Fe_3(BO_3)_4$ [8]. The best agreement is achieved for the following set of the crystal-field parameters $\left(B_q^k,\ \text{in cm}^{-1}\right)$:

$$B_0^2 = 450,\ B_0^4 = -1550,\ B_3^4 = 860,$$
$$B_0^6 = 340,\ B_3^6 = 150,\ B_6^6 = 425. \quad (6)$$

The set of parameters (6) corresponds to the energies of the lower levels of the ground multiplet of the Ho^{3+} and Er^{3+} ions in $Ho_{0.9}Er_{0.1}Fe_3(BO_3)_4$ that are given in table 1 for $B = 0$. These energies are given for $T > T_N$ and with allowance for the *f–d* interaction at $T = 2$ K $< T_N$ (the inclined (INC) state, see below). It can be seen that the inclusion of the *f–d* interaction at $T < T_N$ results in the removal of the degeneracy of the lower levels.

Table 1. Energies of the eight lower levels of the ground multiplets of the Ho^{3+} and Er^{3+} ions in $Ho_{0.9}Er_{0.1}Fe_3(BO_3)_4$ at $B = 0$ that are split by the crystal field (parameters (6)) in the paramagnetic and ordered (with allowance for the *f–d* interaction) temperature ranges.

R	*T*	$\Delta = E_i - E_1$, cm^{-1} (i = 1-8)
Ho	$T > T_N$	0, 0, 7.1, 20.3, 20.3, 62.7, 135, 192
	2 K $< T_N$	0, 5.0, 16.8, 26.6, 30.1, 70, 141, 194
Er	$T > T_N$	0, 0, 28.3, 28.3, 77.3, 77.3, 129, 129
	2 K $< T_N$	0, 5.1, 30.4, 31.8 77.9, 82.3, 130, 133.5

The calculated magnetic characteristics presented below in the figures were calculated for the parameters given in table 2, which also gives the parameters of $HoFe_3(BO_3)_4$ [11] and $ErFe_3(BO_3)_4$ [11] for comparison.

In the calculations, we also use the uniaxial anisotropy constants of iron ($K_2^{Fe} = -2.7$ T·μ_B and $K_4^{Fe} = 0.83$ T·μ_B at $T = 4.2$ K) and the anisotropy constant of iron in the basal plane ($K_{66}^{Fe} = -1.35 \cdot 10^{-2}$ T·μ_B [12]). The K_2^{Fe} and K_4^{Fe} values are consistent with the corresponding uniaxial constants determined when describing the INC state in $Pr_xY_{1-x}Fe_3(BO_3)_4$ [13] and $Ho_{0.5}Nd_{0.5}Fe_3(BO_3)_4$ [8].

To calculate the magnetic characteristics of $Ho_{0.9}Er_{0.1}Fe_3(BO_3)_4$ when an external field is directed along or perpendicular to trigonal axis *c*, we used the schemes of orientation of the magnetic moments of iron $\mathbf{M}_i^{Fe}$ and a rare-earth $\mathbf{m}_i^{R}$ subsystems shown in figure 1.

Figure 2 shows the experimental magnetization curves $M_{a,c}(B)$ of $Ho_{0.9}Er_{0.1}Fe_3(BO_3)_4$ obtained at T = 3–30 K in magnetic fields directed along the trigonal axis (B||c) (figure 2*a*) and in the basal plane (B||a) (figure 2*b*). The characters of magnetization of $Ho_{0.9}Er_{0.1}Fe_3(BO_3)_4$ in the basal plane and along the trigonal axis differ weakly, which indicates a weakly anisotropic contribution of the rare-earth subsystem induced by the crystal-field of the holmium-erbium ferroborate. figure 3 shows the experimental and calculated curves $M_{a,c}(B)$ of $Ho_{0.9}Er_{0.1}Fe_3(BO_3)_4$ at $T = 3$ K and for comparison $M_{a,c}(B)$ curves of $HoFe_3(BO_3)_4$ [14] at $T = 2$ K. As can be seen from figures 2, 3 there are no anomalies on the experimental and calculated magnetization curves $M_c(B)$ of $Ho_{0.9}Er_{0.1}Fe_3(BO_3)_4$ at T = 3–30 K, in contrast to the magnetization curve M_c^{HoFe} of $HoFe_3(BO_3)_4$ [14] at $T = 2$ K, on which a jump of magnetization is clearly visible in the field $B \approx 0.5$ T. The jump in curve M_c^{HoFe} is caused by spin-flop transition in the Fe-subsystem of $HoFe_3(BO_3)_4$ [11].

It can be seen from inset in figure 3 that the experimental curves M_c^{HoFe} (at $B \approx 0.95$ T) and $M_a(B)$ of $Ho_{0.9}Er_{0.1}Fe_3(BO_3)_4$ (at $B \approx 0.2$ T) are characterized by magnetization jumps.

The low-temperature magnetic state of substituted ferroborate $Ho_{0.9}Er_{0.1}Fe_3(BO_3)_4$ is unknown. Our extensive calculations of the magnetic phases that appear in $Ho_{0.9}Er_{0.1}Fe_3(BO_3)_4$ at various orientations of the magnetic moments of the Ho-, Er- and Fe-subsystems suggest the presence of a low-temperature

state that differs from both the EP and the EA states. An antiferromagnetic phase with the magnetic moments of iron deviating from axis *c* through an angle $\theta \approx 65.5°$ (at $T = 2$ K) appears; as a result, a cone of easy magnetization axes (inclined state) forms at $B = 0$ (see figure 1*a*). The possible magnetic field-induced intermediate states with a noncollinear antiferromagnetic structure result from the competition of the contributions of the Ho-, Er-, and Fe-subsystems to the total magnetic anisotropy of $Ho_{0.9}Er_{0.1}Fe_3(BO_3)_4$ and Zeeman energy. The magnetic anisotropy of the Er- and Fe-subsystems stabilizes the EP magnetic structure. The Ho-subsystem stabilizes the EA state. As a result, at certain temperatures and fields, the iron magnetic moments can be oriented at angle θ to the *c*-axis. The possible implementation of the initial INC state in ferroborates was experimentally confirmed in the $Pr_xY_{1-x}Fe_3(BO_3)_4$ compounds [15, 13].

Table 2. Parameters of $Ho_{0.9}Er_{0.1}Fe_3(BO_3)_4$ and, for comparison, parameters of $HoFe_3(BO_3)_4$ [11] and $ErFe_3(BO_3)_4$ [11] (the intrachain Fe-Fe exchange field B_{dd1}, the interchain Fe-Fe exchange field B_{dd2}, and the *f–d* exchange field B_{fd} are the low-temperature exchange fields corresponding to the molecular constants λ_1, λ_2, and λ_{fd}, respectively; Δ_{fd} is the low-temperature splitting of the ground state of an R-ion due to the *f–d* interaction in the following states: an inclined (INC) magnetic state, easy-axis (EA) state, and easy-plane (EP) state; T_{SR} is the spin-reorientation transition temperature; T_N is the Neel temperature; Θ is the paramagnetic Neel temperature for the iron subsystem; $M_0 = |M_i(T = 0, B = 0)| = 15\ \mu_B$ is the magnetic moment of iron per formula unit).

$RFe_3(BO_3)_4$	R = Ho	R = $Ho_{0.9}Er_{0.1}$		R = Er
$B_{dd1} = \lambda_1 M_0$, T	68	68		62.5
λ_1, T/μ_B	–4.53	–4.53		– 4.16
$B_{dd2} = \lambda_2 M_0$, T	26	26		26
λ_2, T/μ_B	–1.73	–1.73		–1.73
$B_{fd} = \lambda_{fd} M_0$, T	3.49	3.1 (Ho) 1.3 (Er)		1.3
λ_{fd}, T/μ_B	–0.23	–0.21 (Ho) –0.09 (Nd)		–0.09
$\Delta_{fd} = \mu_B g\lambda_{fd} M_0$,	~ 10.6 (EA)	Ho	~ 5.0 (INC)	~ 5.7
cm^{-1}	~ 9.7 (EP)	Er	~ 5.1 (INC)	(EP)
T_{SR}, K	~ 4.7-5	-		-
θ_1, ° ($B = 0$)	0 ($T < T_{SR}$) 90 ($T > T_{SR}$)	~ 65.5 ($T = 2$ K)		90
T_N, K	~37.4-39	~ 37		~ 37.4
Θ , K	–210	–165		–145

When the trigonal $Ho_{0.9}Er_{0.1}Fe_3(BO_3)_4$ crystal is magnetized in the basal *ab* plane in weak fields, all the three possible domains with the antiferromagnetic axes oriented at an angle of 120° to each other contribute to the magnetization (scheme *c* in figure 1). The $M_a(B)$ curves were calculated using the approach proposed in [12], where the magnetization processes occurring in easy-plane $NdFe_3(BO_3)_4$ were comprehensively studied with allowance for the possible existence of three types of domains. In the critical field $B_{SR} \approx 0.2$ T a spin-flop transition occurs in a domain with an antiferromagnetism axis along axis a L_0 (see schemes *c, d* in figure 1) causing an anomaly of the $M_a(B)$ curve. This anomaly in curve $M_a(B)$ of $Ho_{0.9}Er_{0.1}Fe_3(BO_3)_4$ exhibits smearing related to the presence of a real domain structure and a certain demagnetizing factor.

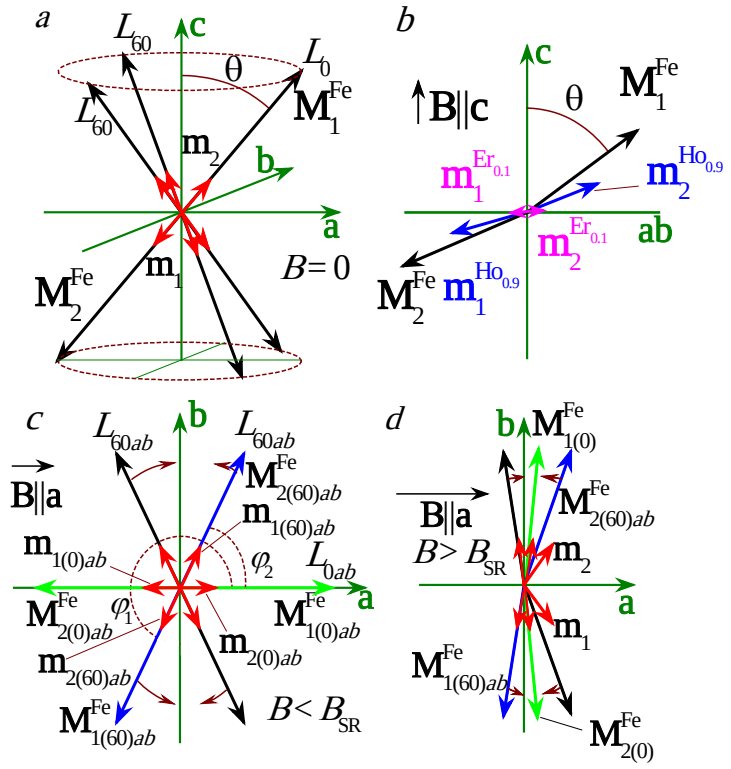

Figure 1. Schemes of orientations of the magnetic moments of the iron and rare-earth $\mathbf{m}_i = \mathbf{m}_i^{Ho_{0.9}} + \mathbf{m}_i^{Er_{0.1}}$ sublattices used in the calculation of the magnetic characteristics for different temperature ranges and different directions of the external magnetic field: (*a*) $B = 0$ (inclined magnetic state), (*b*) **B**||**c** (the *ab* plane is perpendicular to the figure plane), and (*c*, *d*) **B**⊥**c** (the axis *c* is perpendicular to the figure plane).

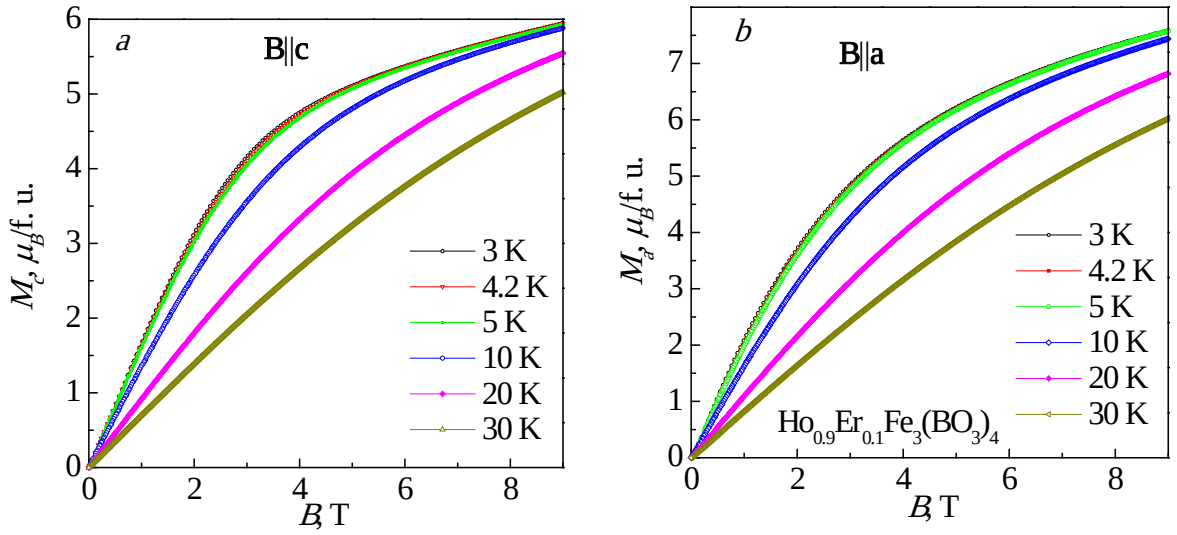

Figure 2. Experimental magnetization curves $M_{a,c}(B)$ of $Ho_{0.9}Er_{0.1}Fe_3(BO_3)_4$ for **B**||**c** (*a*) and **B**||**a** (*b*) at T = 3–30 K.

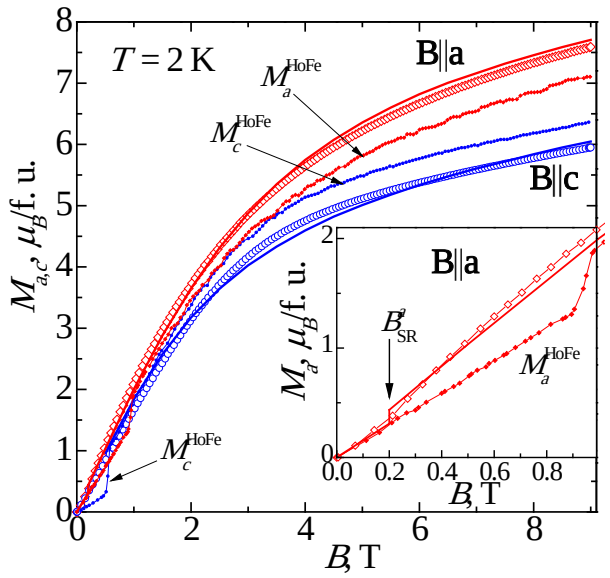

Figure 3. Experimental (symbols) and calculated (lines) magnetization curves $M_{a,c}(B)$ of $Ho_{0.9}Er_{0.1}Fe_3(BO_3)_4$ at T = 3 K. $M_{a,c}^{HoFe}$ - magnetization curve of $HoFe_3(BO_3)_4$ [14] at T = 2 K. Inset: magnetization curves $M_a(B)$ in fields up to 1 T.

It can be seen that figure 4 shows a good agreement between theory and experiment at higher temperature T =10 K.

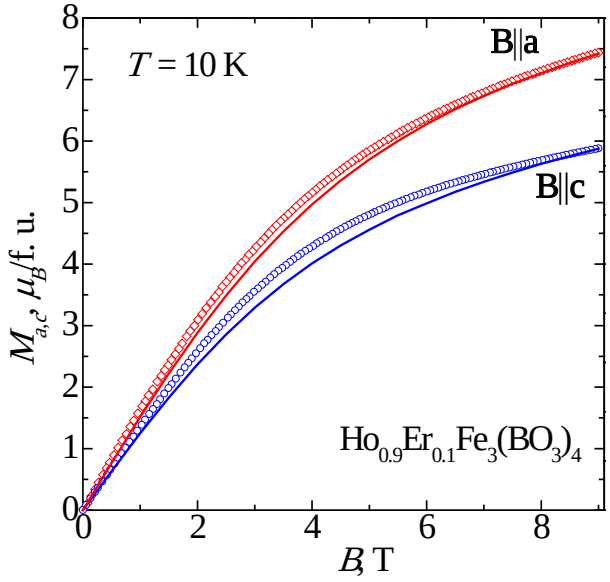

Figure 4. Experimental (symbols) and calculated (lines) magnetization curves $M_{a,c}(B)$ at T = 10 K.

Figure 5 shows the experimental and calculated temperature dependences of the initial magnetic susceptibilities $\chi_{a,c}(T)$ of $Ho_{0.9}Er_{0.1}Fe_3(BO_3)_4$. The weakly anisotropic behavior of the $\chi_{a,c}(T)$ curves is clearly visible. As follows from the inset to figure 5 the experimental magnetic susceptibility $\chi_c^{HoFe}(T)$ of $HoFe_3(BO_3)_4$ [4] near T_{SR} = 4.5 K decreases sharply, that can be explained by the existence of the spin-reorientation transition from the EP state (at $T > T_{SR}$) to EA state (at $T < T_{SR}$). The experimental investigation of the curves $\chi_{a,c}(T)$ showed the absence of a spin-reorientation transition in $Ho_{0.9}Er_{0.1}Fe_3(BO_3)_4$ with the decrease in temperature to 3 K. The calculation of the temperature dependences $\chi_{a,c}(T)$ of $Ho_{0.9}Er_{0.1}Fe_3(BO_3)_4$ with the determined parameters made it possible to establish the absence of a spin-reorientation transition at $T < 3$ K.

The Schottky-type anomaly in the experimental $\chi_{a,c}(T)$ curves near T = 3.5 K is related to the redistribution of the lower levels populations for the ground multiplet of the Ho^{3+} ion in $Ho_{0.9}Er_{0.1}Fe_3(BO_3)_4$ and a correct calculation of the magnetization processes reproduces this effect.

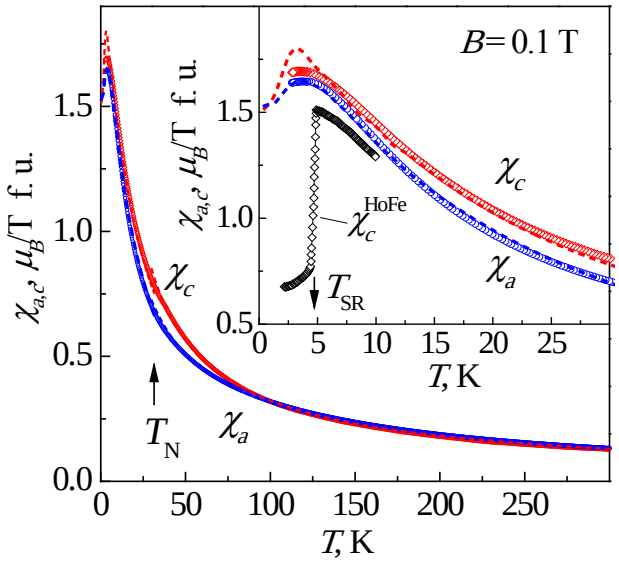

Figure 5. Experimental (symbols) and calculated (lines) temperature dependences of the initial magnetic susceptibility of $Ho_{0.9}Er_{0.1}Fe_3(BO_3)_4$ parallel (χ_c) and perpendicular (χ_a) to the trigonal axis at B = 0.1 T. Inset: low-temperature region of the $\chi_{a,c}(T)$ curves. χ_c^{HoFe} - experimental magnetic susceptibility of $HoFe_3(BO_3)_4$ [4].

Thus, the absence of anomalies in the magnetic characteristics of $Ho_{0.9}Er_{0.1}Fe_3(BO_3)_4$, associated with the spin-orientation transition, is due to the EP contribution of the $Er_{0.1}$-subsystem stabilizes the EP state $Ho_{0.9}Er_{0.1}Fe_3(BO_3)_4$ till lower temperatures than in $HoFe_3(BO_3)_4$.

5. Conclusion

We experimentally and theoretically investigated the magnetic properties of $Ho_{0.9}Er_{0.1}Fe_3(BO_3)_4$ with the competing Ho–Fe and Er–Fe exchange couplings and obtained a good agreement between the theory and experiment for the entire set of the measured characteristics. The single theoretical approach allowed us to determine the important parameters by comparing the calculated data with the experimental results.

During magnetization along axis *a* in a field of about 0.2 T, a spin-flop transition in one of the three possible domains resulting from trigonal symmetry causes the shape of the $M_a(B)$ curves that is characteristic of a phase transition smeared under real domain structure conditions.

The experimental and theoretical investigation of the temperature dependences of the magnetic susceptibility $\chi_{a,c}(T)$ showed the absence of a spin-reorientation transition in $Ho_{0.9}Er_{0.1}Fe_3(BO_3)_4$ with the decrease in temperature to 3 K. The Schottky-type anomaly in the experimental $\chi_{a,c}(T)$ curves near T = 3.5 K is related to the redistribution of the lower levels populations for the ground multiplet of the Ho^{3+} ion in $Ho_{0.9}Er_{0.1}Fe_3(BO_3)_4$ and a correct calculation of the magnetization processes reproduces this effect.

The absence of anomalies in the magnetic characteristics of $Ho_{0.9}Er_{0.1}Fe_3(BO_3)_4$, associated with the spin-orientation transition, is due to the EP contribution of the $Er_{0.1}$-subsystem stabilizes the EP state $Ho_{0.9}Er_{0.1}Fe_3(BO_3)_4$ till lower temperatures than in $HoFe_3(BO_3)_4$.

Acknowledgments

This study was supported by the Russian Foundation for Basic Research, project no. 17-52-45091 IND_a.

References

[1] Kadomtseva A M, Popov Yu F, Vorob'ev G P, Pyatakov A P, Krotov S S, Kamilov K I, Ivanov V Yu, Mukhin A A, Zvezdin A K, Kuz'menko A M, Bezmaternykh L N, Gudim I A and Temerov V L 2010 *Low Temp. Phys*. **36** 511

[2] Popova E A, Volkov D V, Vasiliev A N, Demidov A A, Kolmakova N P, Gudim I A, Bezmaternykh L N, Tristan N, Skourski Yu, Buechner B, Hess C and Klingeler R 2007 *Phys. Rev.* B **75** 224413

[3] Popov Yu F, Kadomtseva A M, Vorob’ev G P, Mukhin A A, Ivanov V Yu, Kuz’menko A M, Prokhorov A S, Bezmaternykh L N and Temerov V L 2009 *JETP Lett*. **89** 345
[4] Chaudhury R P, Yen F, Lorenz B, Sun Y Y, Bezmaternykh L N, Temerov V L and Chu C W 2009 *Phys. Rev.* B **80** 104424
[5] Demidov A A, Gudim I A and Eremin E V 2012 *JETP* **114** 259
[6] Ritter C, Vorotynov A, Pankrats A, Petrakovskii G, Temerov V, Gudim I and Szymczak R 2008 *J. Phys.: Condens. Matter* **20** 365209
[7] Popova E A, Vasiliev A N, Temerov V L, Bezmaternykh L N, Tristan N, Klingeler R and Buchner B 2010 *J. Phys.: Condens. Matte.* **22** 116006
[8] Gudim I A, Demidov A A, Eremin E V and Shukla D K 2018 *Phys. Sol. State* **60** 1989
[9] Bezmaternykh L N, Temerov V L, Gudim I A and Stolbovaya N A 2005 *Crystallogr. Rep*. **50** S97
[10] Gudim I A, Eremin E V and Temerov V L 2010 *J. of Cryst. Growth* **312** 2427
[11] Demidov A A 2016 *Extended Abstract of Doctoral Dissertation* (Moscow: Moscow State Univ.)
[12] Volkov D V, Demidov A A and Kolmakova N P 2007 *J. Exp. Theor. Phys*. **104** 897
[13] Pankrats A I, Demidov A A, Ritter C, Velikanov D A, Semenov S V, Tugarinov V I, Temerov V L and Gudim I A 2016 *J. Phys.: Condens. Matter* **28** 396001
[14] Pankrats A, Petrakovskii G, Kartashev A, Eremin E and Temerov V 2009 *J. Phys.: Condens. Matter* **21** 436001
[15] Ritter C, Pankrats A I, Demidov A A, Velikanov D A, Temerov V L and Gudim I A 2015 *Phys. Rev.* B **91** 134416